Chapter 12
Influence of C–O–H–Cl-Fluids on Melting Phase Relations of the System Peridotite-Basalt: Experiments at 4.0 GPa

N. S. Gorbachev, A. V. Kostyuk, P. N. Gorbachev, A. N. Nekrasov, and D. M. Soultanov

Abstract The article presents the results of experiments at pressure 4.0 GPa and temperature 1400 °C on the influence of fluids (H_2O, $H_2O + CO_2$, $H_2O + HCl$) on the composition of restite and magma formed during the melting of the peridotite-basalt-$(K, Na)_2CO_3$ system as a model analogue of the mantle reservoir contaminated with protoliths of subducted oceanic crust. The composition of the fluid has a significant impact on the phase relations. In "dry" conditions and with H_2O fluid alkaline melts of phonolite type are formed, at $H_2O + CO_2$ fluid composition—trachiandezybasalts, with $H_2O + HCl$ fluid—riodacite melts. The alkaline melts coexist with an olivine-free restite pyroxene-phlogopite composition. Critical relations between fluid and silicate melt are observed in the water-bearing system. Interaction of supercritical fluid melts with peridotite restite leads to the formation of clinopyroxene, K-amphibole, phlogopite, carbonate, quenching silicate globules. Newly formed clinopyroxene and K-amphibole are in reactionary relations with olivine, orthopyroxene and clinopyroxene of peridotite restite. The revealed effects testify to instability of olivine at melting of peridotite-basalt mixture in the presence of fluid, effective influence of fluid composition on phase composition and critical ratios.

Keywords Experiment · Mantle · Crust · Fluid · Melt · Interaction · Melting · Critical relations

12.1 Introduction

The most important mechanism of large-scale exchange of matter between the crust and mantle is the subduction of the oceanic crust, leading to the eclogitization of basalts and the formation of reservoir in the mantle with protoliths of the subducted crust (Taylor and Neal 1989). The volatile enriched fluid has an effective effect on the phase composition, melting point of the mantle, the composition of the formed

N. S. Gorbachev (✉) · A. V. Kostyuk · P. N. Gorbachev · A. N. Nekrasov · D. M. Soultanov
D.S. Korzhinskii Institute of Experimental Mineralogy, Russian Academy of Science, Academician Osipyan Street 4, Chernogolovka, Moscow Region, Russia 142432
e-mail: gor@iem.ac.ru

Y. Litvin and O. Safonov (eds.), *Advances in Experimental and Genetic Mineralogy*, Springer Mineralogy, https://doi.org/10.1007/978-3-030-42859-4_12

fluid-containing silicate and salt (carbonate, chloride, sulfide) melts. High extracting and transport properties of fluids at high pressures lead to mobilization and transport of main and impurity elements. The processes of mantle metasomatism are related to their interaction with the mantle substrate.

The experimental model of the mantle reservoir with protoliths of the subducted oceanic crust is the system of peridotite-basalt-fluid. This type of system has been experimentally studied under "dry" conditions (Yaxley 2000; Tumiati et al. 2013; Mallik and Dasgupta 2012). Fluid-containing systems have been studied to a lesser extent. The system of peridotite-basalt in the presence of water and water-carbonate fluids was studied experimentally in the interval of 1250–1400 °C, 1.5–2.5 GPa (Gorbachev 1990). Instability of olivine in the presence of water-containing fluid was revealed. It is shown that the formation of magnesia magmas of the picritobasalt type does not require overheating of the mantle, their formation occurs at temperatures close to the mantle adiabatic point (Gorbachev 2000).

An important feature of fluid-containing silicate systems is the existence of critical relations between silicate melt and fluid at high pressures and temperatures, caused by their high mutual solubility. At critical $P_C T_C$, there is a complete mixing between them with the formation of supercritical fluid melt, and in the 2nd end critical point ($2P_C T_C$) with the equality of P-T silicate solidus and $P_C T_C$ equilibrium melt fluid—a complete mixing between the liquidus phases, melt and fluid, which makes it difficult to determine P-T silicate solidus (Keppler and Audetat 2005; Litasov and Ohtani 2007).

The existence in the upper mantle of critical relations and composition of supercritical fluids-melt is proved by fluid-melt inclusions in diamonds, in minerals of mantle xenoliths of peridotite and eclogites from kimberlites and alkaline basalts, as well as in tectonically embedded carbonate-containing peridotite and eclogite massifs. Three main final types of such fluids are distinguished: carbonate enriched with Ca, Mg, Fe; salt enriched with Na, K, H_2O and silicate enriched with Si, Al (Klein-Bendavid et al. 2007; Navon et al. 1988; Weiss et al. 2009; Bogatikov et al. 2010). There is a complete mixture between alkaline and carbonate, carbonate and silicate end compositions of mantle fluids, and at pressure and temperature of the second critical point—between silicates and fluid (Wyllie and Ryabchikov 2000; Kessel et al. 2005).

Critical ratios were experimentally studied in water-containing silicate systems of monomineral (SiO_2, albite, nepheline, jadeite) and granite compositions. In these systems the critical pressure and temperature of $P_C T_C$ and $2P_C T_C$ lie in the range of 0.7–2.3 GPa, 550–1050 °C, increasing in the sequence of quartz–nepheline–albite–jadeite–granite. Critical pressures decrease when components (e.g. fluorine) are added to the fluid, increasing the mutual solubility of the melt and fluid, and increase when a component is added to the fluid, reducing the mutual solubility of the melt and fluid (e.g. CO_2) (Bureau and Keppler 1999). It has been established that at $H_2O + CO_2$ composition of the fluid in the system of peridotite-basalt critical ratios of silicate melt—fluid do not occur up to pressures of 4 GPa, but are observed at the water composition of the fluid. It was shown that 4 GPa and 1400 °C in the system of peridotite-basalt-H_2O characterize parameters of the 2 end critical points (Gorbachev 2000).

In the main and ultrabasic systems, much attention was paid to the $P_C T_C$ of the second end critical point of $2P_C T_C$. In the Fo–En–H_2O system, $2P_C T_C$ pressure is estimated at 12–13 GPa (Stalder et al. 2001), eclogite-H_2O at 5–6 GPa (Kessel et al. 2005), basalt-peridotite-H_2O at 3.8–4.0 GPa (Gorbachev 2000), and peridotite-H_2O at 3.8 GPa (Mibe et al. 2007). The Fo + En + H_2O + CO_2 $2P_C T_C$ system is estimated at 12–15 GPa (Willy and Rhyabchikov 2000). Critical ratios also exist between silicate and carbonate melts (Kisseva et al. 2012; Dasgupta et al. 2005; Gorbachev et al. 2015a, b).

In the majority of experimental works the transition of the system to the supercritical state and critical equilibria of melt and fluid were determined in situ at extreme (supra-liquidus) temperatures. The complete melt and fluid miscibility has been recorded either visually or by the homogenization of the 2-phase melt fluid association on diamond anvil equipment (Bureau and Keppler 1999) or by X-ray radiography (X-ray radiography) (Mibe et al. 2007). In some studies, the quenching method was used, where the transition from subcritical to supercritical state in the eclogite-H_2O system was fixed by the composition of quenching water-bearing glass and fluid in diamond traps (Kessel et al. 2005). However, these methods do not allow us to study the peculiarities of the phase composition in the interaction of supercritical fluid melts with restite. Moreover, most of the experiments were carried out at extreme temperatures. Taking into account the large temperature interval between solidus and liquidus in the main and ultrabasic systems, as well as the formation of mantle magmas in the partial melting of the mantle substance, it is of great interest to study the critical relations between partial (subliquidus) melts and fluid in the presence of refractory restite. In the works (Gorbachev 2000; Gorbachev et al. 2015a, b), the texture and phase composition of experimental samples can be used as a critical ratio test in such experiments. The composition of supercritical fluid melts and the nature of their interaction with the silicate substrate depend on the ratio of silicate and fluid components. It is believed that at intermediate compositions in supercritical fluid melts there may exist clusters, typical for both melt and fluid (Wyllie and Rhyabchikov 2000). The dual nature of supercritical fluid melts may appear in the structure and phase composition of the material formed during quenching after the experiment.

To obtain new data on the influence of fluid composition on melting, phase composition and critical ratios in the fluid-containing upper mantle, the system of peridotite-basalt-$(Na, K)_2CO_3$ under “dry” conditions and in the presence of H_2O, $H_2O + CO_2$ and H_2O + HCl fluids is studied at $P = 4$ GPa, $T = 1400$ °C as an experimental model of a mantle reservoir with protoliths of subducted oceanic crust.

12.2 Experiment

The experiments were carried out in IEM RAS on the anvil with hole apparatus (NL-40) using a multi-ampoule technique with a Pt-peridotite ampoule (Gorbachev 1990). A specially prepared peridotite ampoule was filled with a mixture of powders of tholeiite basalt and sodium and potassium carbonates. Start composition (wt%): peridotite—55 wt%, basalt—25 wt%, sodium and potassium carbonate ~10 wt%. Chemical compositions of peridotite and basalt are given in Table 12.1. The source of fluids (20 wt% versus silicate) was distilled H_2O, oxalic acid dihydrate $H_2C_2O_4 \times 2H_2O$, 1H solution HCl. Chromite was added as accessory minerals, and Ni–Cu–Pt containing pyrrhotite was used in experiments under "dry" conditions. The charged peridotite ampoule was placed in a "working" Pt ampoule ($d = 5$ mm), which was hermetically welded. This ampoule was placed in a larger Pt ampoule ($d = 10$ mm) containing a fO_2 buffer association close to the quartz-fayalite-magnetite buffer. Temperature was measured by Pt30Rh/Pt6Rh thermocouple, pressure at high temperatures was calibrated according to the quartz-coesite equilibrium curve. The accuracy of the temperature and pressure tests is estimated at ±5 °C and ±1 kbar (Litvin 1991). The duration of the experiment was 18–24 h. The products of the experiments—polished preparations of quenching samples—were studied on the electronic scanning microscope CamScan MV2300 with YAG detector of secondary and reflected electrons and energy dispersive X-ray microanalyzer with semiconductor Si(Li) detector Link INCA Energy.

12.3 Results

12.3.1 Peridotite-Basalt-Na_2CO_3–K_2CO_3 System

Microphotographs of quenching samples are given in Fig. 12.1, chemical compositions of coexisting phases are given in Table 12.2. In "dry" conditions the quenched samples inherit the structure of peridotite ampoule. The inner "basalt" part, the "reaction" zone at the contact basalt-peridotite and the outer "peridotite" part of the ampoule are separated. The texture is massive. Although there was no disintegration of the initial peridotite ampoule during the experiment, the mineral composition of the zones is similar as a result of the reactions occurring during the experiment. Their main resemblance is the absence of olivine. The samples consist of isolated secretions of pyroxenes, phlogopite, chromium-spinel, cemented with intergranular alkaline melt (Table 12.2, Fig. 12.1b, c). Pyroxene grains of 20–50 μ in size have a zonal structure. The reaction relations of clinopyroxene ← orthopyroxene in the peridotite part of the sample are observed. The central part of the crystal is characterized by a higher content of MgO (up to 33 wt%), low content of CaO (~3 wt%) is represented by orthopyroxene. The edges of the grain are lighter colored due to a decrease in the concentration of MgO (up to 20–22 wt%) and an increase in the

Table 12.1 Chemical compositions (in wt%) of the initial peridotite and basalt in experiments

Peridotite														
SiO_2	TiO_2	Al_2O_3	Cr_2O_3	FeO	MnO	MgO	CaO	Na_2O	K_2O	P_2O_5	H_2O^-	H_2O^+	LOI[a]	Total
42.84	0.04	1.74	0.56	7.19	0.13	40.52	3.39	0.12	0.03	0.02	0.41	2.00	1.00	100.0
Basalt														
50.02	1.85	14.51	–	14.03	0.20	5.85	10.40	2.50	0.72	–	–	–	–	100.08

Note [a]LOI—loss on ignition

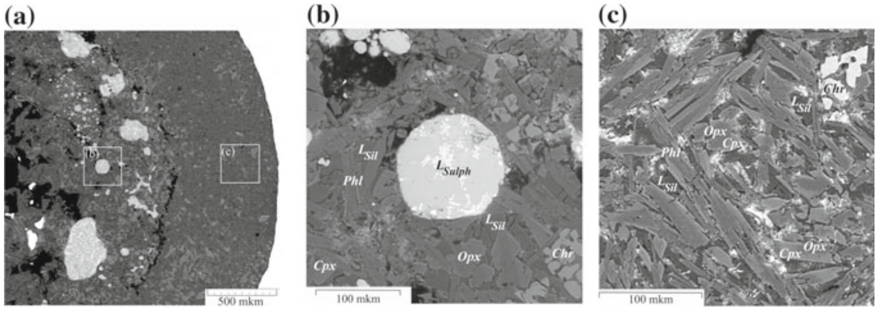

Fig. 12.1 *Peridotite-basalt-Na_2CO_3–K_2CO_3 system.* BSE images of experimental run products. **a** General view of the sample consist of peridotite ampoule and basalt; **b** phase composition of reaction zone consist of: orthopyroxene (*Opx*), clinopyroxene (*Cpx*), phlogopite (*Phl*), chromite (*Chr*), with inclusions of sulphide globules (L_{Sulph}), cemented by alkaline silicate glass (L_{Sil}); **c** peridotite ampoule consist of orthopyroxene (*Opx*), clinopyroxene (*Cpx*), phlogopite (*Phl*) and chromite (*Chr*), cemented by alkaline silicate glass (L_{Sil})

content of CaO (up to 12–14 wt%), belong to the pigeonites (Fig. 12.1c, Table 12.2). In the reaction zone of the ampoule isolated orthopyroxene crystals coexist with clinopyroxenes of avgite composition. Silicate melt has a phonolite composition. SiO_2 content ~55 wt%, $K_2O + Na_2O$ ~ 11–13 wt%, K_2O/Na_2O ~ 0.15. Sulfides are concentrated in the reaction zone. The oval, molten form of sulfides indicates partial melting of the original pyrrhotite. Sulfide globula matrix is represented by Fe–Ni sulfide of pentlandite and Ni-pyrrhotite composition with inclusions of PtS and Pt–Fe phase (Table 12.2, Fig. 12.1b).

12.3.2 Peridotite-Basalt-Na_2CO_3–K_2CO_3–($H_2O + CO_2$) System

Microphotographs of the samples are shown in Fig. 12.2, chemical compositions of the coexisting phases-in Table 12.3. The hardened sample has a solid texture. The initial structure of the peridotite ampoule is not preserved. The texture and phase composition of peridotite and its basaltic part are similar. The experimental sample consists of clinopyroxene, K-clinopyroxene, phlogopite, single grains of orthopyroxene. Notice the absence of olivine among restite minerals. Klinopyroxene is moderately aluminous (up to 9 wt% Al_2O_3), concentration of micro impurities TiO_2, Cr_2O_3 does not exceed 0.5 wt%, Na_2O content is about 0.8 wt%. Potassium clinopyroxene is more aluminous (up to 12 wt% Al_2O_3), with a reduced concentration of SiO_2 (46–47 wt%), concentration of micro impurities does not exceed 0.5 wt% for TiO_2 and 0.7 wt% for Cr_2O_3, enriched with Na_2O (up to 2.5 wt%), K_2O (up to 0.7 wt%), ratio of K_2O/Na_2O ~ 0.3. Phlogopite is found in the form of thin, filiform secretions.

Table 12.2 Chemical compositions (in wt%) of coexisting phases in peridotite–basalt–(Na, K)$_2$CO$_3$ system

	SiO_2	TiO_2	Al_2O_3	FeO	MnO	MgO	CaO	Na_2O	K_2O	Cr_2O_3	SO_3	Total
Peridotite-basalt contact												
Opx	54.99	0.39	5.99	2.59	0.25	32.86	3.27	0.99	0.27	0.84	0.57	103.63
Cpx	51.05	0.66	5.61	2.09	0.25	16.46	17.57	1.87	0.00	0.67	0.31	96.54
Phl	40.77	0.50	13.11	1.24	0.00	25.54	0.13	1.25	8.03	1.94	0.48	93.85
Cht	0.30	0.32	16.61	5.90	0.57	20.03	0.00	0.26	0.15	54.95	0.04	99.99
L_{Sil}	55.02	0.40	19.18	0.46	0.07	0.00	0.63	9.92	1.52	0.02	0.29	87.50
Peridotite part												
Opx	54.23	0.47	5.06	2.61	0.03	30.40	3.93	0.53	0.04	1.35	0.00	98.66
Cpx	54.16	0.61	5.00	2.56	0.31	21.53	13.43	1.20	0.00	0.88	0.01	99.67
Phl	41.53	0.66	12.71	1.91	0.09	25.49	0.89	1.10	7.37	1.41	0.00	93.15
Cht	0.26	0.21	18.36	7.17	0.55	18.62	0.10	0.57	0.00	50.43	0.69	97.49
L_{Sil}	55.97	0.33	19.20	0.68	0.17	0.21	0.50	10.75	1.52	0.00	0.08	89.40

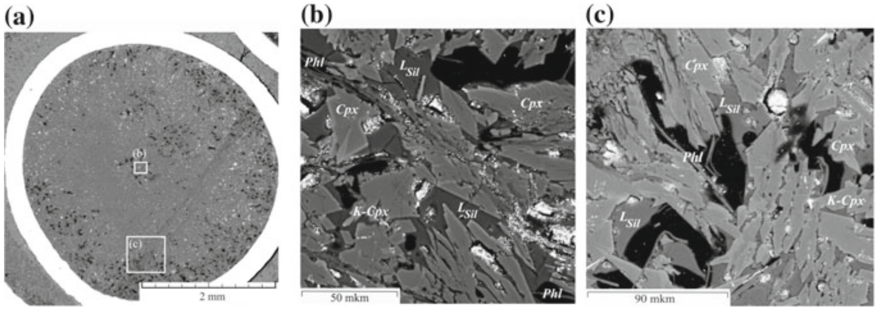

Fig. 12.2 *Peridotite-basalt-Na_2CO_3–K_2CO_3–(H_2O + CO_2) system.* BSE images of experimental run products. **a** General view of the sample. During melting, the composition averaged. Contact between the peridotite and basalt parts is almost not observed; **b** basalt, **c** peridotite part of the ampoule. Their texture and phase composition (Ca-clinopyroxene (*Cpx*), K-clinopyroxene (*K-Cpx*), phlogopite (*Phl*) and intergranular silicate glass (L_{Sil})) are similar

Silicate melt of moderate alkalinity refers to trachiandezybasalts. The alkali content in the melt ($K_2O + Na_2O$) is about 6 wt%, Na_2O/K_2O ~ 2.3.

12.3.3 Peridotite-Basalt-Na_2CO_3–K_2CO_3–H_2O System

Microphotographs of the samples are shown in Fig. 12.3, chemical compositions of coexisting phases-in Table 12.4.

Disintegration of the peridotite ampoule was observed in the experimental products. As can be seen in Fig. 12.3a, the cross section of the sample only shows the components of the initial sample: disintegrated peridotite ampoule (Fig. 12.3c), reaction zone on the border of peridotite-basalt and "basalt" (Fig. 12.3b, c) the part of the initial sample formed during the quenching of supercritical fluid-melt consisting of a mixture of small crystals (up to 5 μ) of silicates, carbonates, sulfide and aluminosilicate microglobules. In contrast to subcritical conditions, massive silicate glass is not formed in the peridotite of the ampoule. The experimental sample consists of isolated relics or intergrowths of peridotite restite (olivine + orthopyroxene + clinopyroxene). Reaction relations between them and newly formed minerals with the replacement of type: orthopyroxene ← clinopyroxene ← K-amphibole (Fig. 12.3d, e), as well as the formation of newly formed and quenched phases—phlogopite, carbonate, Al–Si globules of phonolite glass (Fig. 12.3f). Figure 12.3(d–f) shows the types of reaction relations in peridotite restite, and Table 12.4 shows their chemical composition.

Table 12.3 Chemical compositions (in wt%) of coexisting phases in peridotite–basalt–(Na, K)$_2$CO$_3$–(H$_2$O + CO$_2$) system

	SiO_2	TiO_2	Al_2O_3	FeO	MnO	MgO	CaO	Na_2O	K_2O	Cr_2O_3	SO_3	Total
Basalt part												
L_{Sil}	53.00	0.14	17.94	0.56	0.00	0.23	3.92	3.38	1.51	0.00	0.00	80.68
K-Cpx	45.72	0.42	11.72	3.78	0.32	19.13	10.08	2.33	0.67	0.67	0.18	95.02
Cpx	50.95	0.47	8.84	4.83	0.17	16.05	16.51	0.84	0.00	0.47	0.00	99.12
Phl	41.35	0.36	14.44	2.94	0.20	22.29	0.06	1.33	6.76	0.38	0.82	91.2
Peridotite part												
L_{Sil}	52.55	0.10	17.32	1.03	0.03	0.25	3.54	3.38	1.45	0.11	0.43	80.2
K-Cpx	46.77	0.43	11.98	3.87	0.33	19.56	10.31	2.38	0.69	0.68	0.18	97.19
Cpx	50.84	0.46	8.82	4.82	0.17	16.02	16.48	0.84	0.00	0.46	0.00	98.92

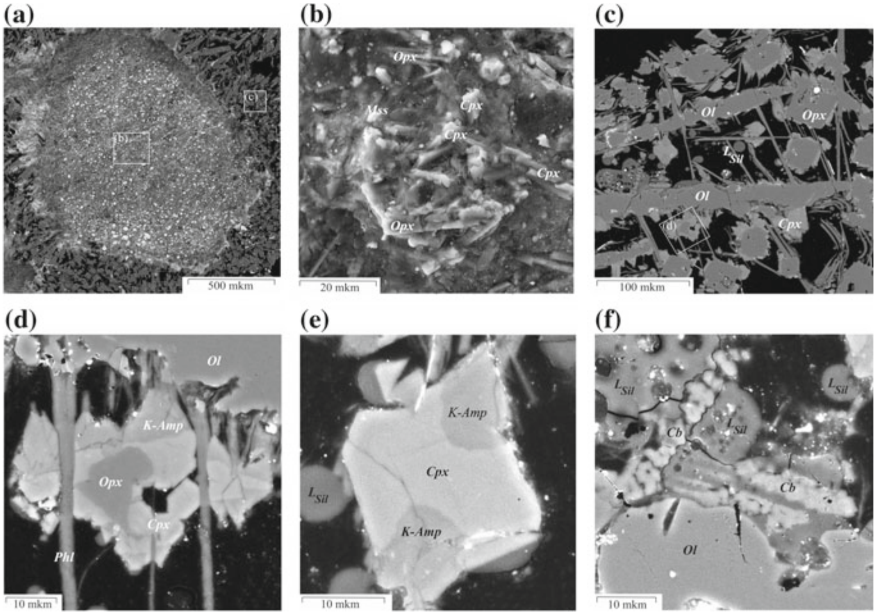

Fig. 12.3 *Peridotite-basalt-Na_2CO_3–K_2CO_3–H_2O system*. BSE images of experimental run products. **a** Peridotite-basalt contact; **b** basalt part, represented by a fine mixture of quenching silicate phases; **c** disintegrated peridotite part; **d**–**f** different areas of peridotite ampoules, characterizing the features of the phase composition, due to the reaction ratios in the peridotite restead with *Opx* ← *Cpx* ← K-*Amp* substitutions, newly formed *Phl*, *Cb* and quenched glass globules (L_{Sil})

12.3.4 Peridotite-Basalt-Na_2CO_3–K_2CO_3–(H_2O + HCl) System

Microphotographs of quenching samples are shown in Fig. 12.4, chemical compositions of coexisting phases-in Table 12.5. The texture and phase composition of the quenching sample resembles that of the $H_2O + CO_2$ fluid experiment (Fig. 12.3). They differ in the presence of halite, riodacite composition of intergranular and quenched (in the form of Al–Si globules) melts. The matrix of experimental samples consists of relics and aggregates of restite minerals clinopyroxene, olivine, orthopyroxene, phlogopite.

Table 12.4 Chemical compositions (in wt%) of coexisting phases in peridotite–basalt–(Na, K)$_2$CO$_3$–H$_2$O system

	SiO_2	TiO_2	Al_2O_3	FeO	MnO	MgO	CaO	Na_2O	K_2O	Cr_2O_3	SO_3	Total
Ol	40.23	0.40	0.78	6.08	0.12	50.20	0.18	0.38	0.04	2.36	0.17	100.75
K-Amp	41.78	0.85	15.02	6.56	0.21	14.36	10.87	2.09	1.50	0.10	0.23	93.62
Cpx	49.11	0.61	8.34	4.16	0.23	16.00	19.69	1.07	0.00	0.00	0.00	99.20
Opx	54.29	0.28	4.88	3.54	0.13	33.33	1.69	0.00	0.00	1.03	0.06	99.23
Phl	40.67	0.35	14.20	2.89	0.20	21.92	0.06	1.31	6.65	0.37	0.81	89.70
L_{Sil}- *glob*	53.08	0.24	18.60	0.10	0.12	0.00	0.22	6.81	2.83	0.04	0.13	82.30
L_{Cb}	6.04	0.10	2.31	1.14	0.51	3.26	40.41	0.61	0.73	0.02	0.11	55.25
Coexisting phases on the Fig. 12.3d												
K-Amp	42.45	0.63	14.52	7.44	0.21	15.56	10.22	2.73	0.95	0.23	0.16	95.66
Cpx	47.71	1.57	8.70	3.00	0.35	14.08	21.33	0.95	0.02	0.52	0.08	98.41
Opx	53.50	0.14	5.23	3.31	0.19	33.20	1.45	0.09	0.06	1.68	0.02	98.91
Phl	41.82	0.29	13.09	2.62	0.00	24.52	0.00	0.84	7.85	0.55	0.00	91.70
Ol	40.23	0.40	0.78	6.08	0.12	50.20	0.18	0.38	0.04	2.36	0.17	100.9
Coexisting phases on the Fig. 12.3e												
K-Amp	41.56	1.15	15.54	6.80	0.15	15.41	10.91	2.91	1.42	0.00	0.20	96.08
Cpx	46.17	0.97	12.51	5.02	0.40	11.82	20.63	1.23	0.07	0.19	0.27	99.48
L_{Sil}- *glob*	52.31	0.01	18.11	0.07	0.00	0.04	0.18	5.76	2.71	0.00	0.08	79.27
Coexisting phases on the Fig. 12.3f												
Ol	40.23	0.40	0.48	6.08	0.12	50.20	0.18	0.38	0.04	2.36	0.17	100.75
L_{Sil}- *glob*	52.70	0.01	17.77	0.09	0.00	0.14	0.20	5.11	2.67	0.00	0.06	78.94
Cb	1.29	0.18	0.78	1.17	0.53	3.46	43.02	0.89	0.13	0.00	0.01	51.47
L_{Sil}	51.21	0.24	18.56	0.21	0.13	0.20	0.46	6.34	2.79	0.02	0.15	80.48

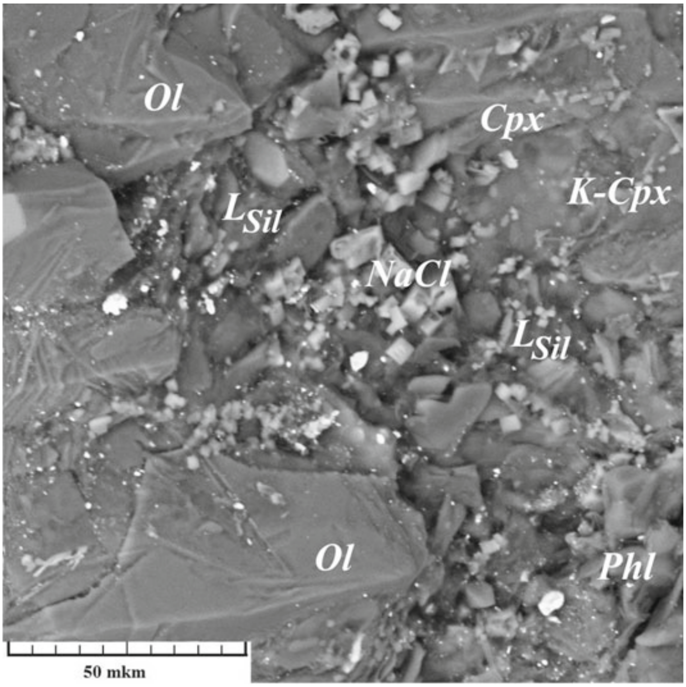

Fig. 12.4 *Peridotite-basalt-Na_2CO_3–K_2CO_3–(H_2O + HCl) system.* BSE image of experimental run products. The formation of NaCl crystals in a silicate matrix consisting of olivine (*Ol*), clinopyroxene (*Cpx*, K-*Cpx*), phlogopite (*Phl*), silicate melt (L_{Sil})

12.4 Discussion

12.4.1 Peridotite-Basalt-Na_2CO_3–K_2CO_3 System

Partial melting of the original sample is observed. Although after the experiment the structure of peridotite ampoule is preserved, but as a result of reactions occurring during the experiment, the mineral composition of peridotite and basalt is similar. Their main feature is the absence of olivine, formation of alkaline melt of phonolite composition, concentration of sulfide melt in the reaction zone. Reaction ratios in pyroxenes of the type of pigeonite ← orthopyroxene is observed in the peridotite part of the ampoule enriched with MgO.

Table 12.5 Chemical compositions (in wt%) of coexisting phases in peridotite–basalt–(Na, K)$_2$CO$_3$–(H$_2$O + HCl) system

	SiO_2	TiO_2	Al_2O_3	FeO	MnO	MgO	CaO	Na_2O	K_2O	Cr_2O_3	SO_3	Total
L_{Sil}	71.45	0.20	18.76	0.59	0.21	2.08	2.82	1.95	1.65	0.00	0.00	99.71
Ol	40.57	0.90	0.59	8.20	0.37	46.82	0.00	0.16	0.05	2.24	0.07	99.97
Cpx	50.72	0.70	9.98	3.85	0.44	15.69	18.27	0.89	0.04	0.86	0.06	101.5
K-Cpx	46.75	0.49	12.69	3.63	0.00	19.72	10.32	2.38	0.68	0.66	0.05	97.42
Phl	41.55	0.31	12.88	2.35	0.41	23.46	0.18	1.56	7.01	0.88	0.16	90.78

12.4.2 Peridotite-Basalt-Na_2CO_3–K_2CO_3–(H_2O + CO_2) System

In the case of partial melting of the initial sample, the structure of the initial peridotite ampoule is not preserved. The phase relations were determined by reactions between the fluid, alkaline fluid-containing melt and peridotite. As a result of reactions, olivine is dissolved, clinopyroxene, K-amphibole, and phlogopite are formed that coexist with the trachiandezybasalt melt.

12.4.3 Peridotite-Basalt-Na_2CO_3–K_2CO_3–H_2O System

At 4 GPa, 1400 °C, critical relations between the carbonated silicate melt and the fluid were achieved. This is evidenced by the peculiarities of texture and phase composition of the samples: disintegration of peridotite of the ampoule, absence of intergranular silicate glass in peridotite. Peridotite ampoule, which was filled with a mixture of basalt and carbonates during the assembly of the initial sample, after the experiment consisted of a compressed mixture of micron-sized particles of silicate and carbonate composition, formed during the quenching of fluid-melt. Reaction relations in restite with substitutions of olivine $\leftarrow$ orthopyroxene $\leftarrow$ clinopyroxene $\leftarrow$ K-amphibole are determined by the interaction with supercritical fluid-melt. Wide development of reaction relations among minerals of peridotite restite testifies to high chemical activity of supercritical fluid-melt. The presence of quenching phases—phlogopite, Al–Si globules, carbonate—characterize the composition of supercritical fluid-melt. At melting of the supercritical mantle reservoir with protoliths of the subducted oceanic crust at *P-T*, exceeding the critical values, there should also be observed decompaction of the substrate as a result of disintegration of peridotite.

12.4.4 Peridotite-Basalt-Na_2CO_3–K_2CO_3–(H_2O + HCl) System

The quenching samples do not inherit the structure of the peridotite ampoule. At partial melting as a result of reactions between peridotite restite, fluid and fluid-containing melt there was an averaging of phase composition of peridotite and basalt components of the initial sample, formation without olivine association coexisting with riodacite melt. The texture and phase composition of the quenched samples are similar to the samples from the experiments with $H_2O + CO_2$ fluid. The formation of halite is observed.

12.4.5 K-Containing Phases

In experiments with $H_2O + CO_2$, $H_2O + HCl$ fluids, potassium phases are represented by K-containing clinopyroxenes with a similar chemical composition. In experiments with aqueous potassium-rich fluids, the K-amphibole phase is represented. Compared to K-clinopyroxene, K-amphibole is depleted in Na, Mg, Si and contains higher concentrations of K, Fe, Al, Ti (Table 12.6).

12.5 Conclusions

The composition of the fluid has a significant influence on the phase composition and critical ratios in mantle reservoirs with protoliths of the oceanic crust. In "dry" conditions and at acid composition of fluid alkaline melts of Na series are formed. The effect of acid-base interaction is clearly manifested, acidification of the fluid shifts the composition of the melt from trachiandezybasalt at $H_2O + CO_2$ composition of the fluid to riodacites with $H_2O + HCl$ fluid. Alkaline melts coexist with non-olivine metasomatically altered restite of pyroxene-phlogopite composition.

Instability of olivine at partial melting of peridotite-basalt mixture in the presence of acid fluid is established. The interaction of fluid and fluid-containing melts with restite in experiments with acid fluid ($H_2O + CO_2$, $H_2O + HCl$) was accompanied by pyroxenization and phlogopitization of peridotite:

$$\begin{aligned} &\mathrm{Mg_2SiO_4}(Ol) + \mathrm{MgSiO_3}(Opx) + (\mathrm{3CaCO_3} + \mathrm{4SiO_2})(L_{Sil} + Fl) \\ &= \mathrm{3CaMgSi_2O_6}(Cpx) + \mathrm{3CO_2}(Fl); \end{aligned}$$

$$\begin{aligned} &\mathrm{2Mg_2SiO_4}(Ol) + \mathrm{2MgSiO_3}(Opx) + (\mathrm{K_2O} + \mathrm{Al_2O_3} + \mathrm{2SiO_2} + \mathrm{2H_2O})(L_{Sil} + Fl) \\ &= \mathrm{3CaMgSi_2O_6}(Cpx) + \mathrm{3CO_2}(Fl). \end{aligned}$$

The acid fluid produces K-containing clinopyroxene, the aqueous fluid produces K-containing amphibole, and the $H_2O + HCl$ fluid produces magmatic halite.

Critical relations between fluid and silicate melt are observed in the water-bearing system. Interaction of supercritical fluid melts with peridotite restitis leads to the formation of clinopyroxene, K-amphibole, phlogopite, carbonate, quenching silicate globules. Newly formed clinopyroxene and K-amphibole are in reactionary relations with olivine, orthopyroxene and clinopyroxene of peridotite restitis. Modal metasomatism of the upper mantle under the influence of water-containing supercritical fluid-melt leads to secondary enrichment—"refertilization" of depleted restite of the harzburgite composition, replacement of peridotite olivine-orthopyroxene association of newly formed phlogopite-clinopyroxene association. The texture and phase composition of the samples under supercritical conditions allow us to draw a conclusion about the zonal structure of reservoirs with protoliths of the subducted oceanic

Table 12.6 Chemical compositions (in wt%) of K-containing phases in systems with different fluid ($H_2O + CO_2$, $H_2O + HCl$, H_2O)

Phase	Fluid	SiO_2	TiO_2	Al_2O_3	FeO	MnO	MgO	CaO	Na_2O	K_2O	Cr_2O_3	SO_3	Total
K-Cpx	$H_2O + CO_2$	46.77	0.43	11.98	3.87	0.33	19.56	10.31	2.38	0.69	0.68	0.18	97.19
K-*Cpx*	$H_2O + HCl$	46.75	0.49	12.69	3.63	0.00	19.72	10.32	2.38	0.68	0.66	0.05	97.42
K-*Amp*	H_2O	41.78	0.85	15.02	6.56	0.21	14.36	10.87	2.09	1.50	0.10	0.23	93.6

crust: the outer zone—metasomatically altered under the influence of supercritical fluid-melt disintegrated restite of dunite or harzburgite composition, underwent “refertilization” as a result of the formation of new minerals in it, the inner zone—isolated lenses of supercritical fluid-melt. Disintegration of fluid-containing mantle peridotite substrate at supercritical pressures can lead to the formation of tectonically weakened zones, fluid paths and upper mantle plumes.

Acknowledgements Acknowledgement. The study was funded by the projects of RFBR №17-05-00930a and IEM RAS №AAAA18-118020590140

References

Bogatikov OA, Kovalenko VI, Sharkov EV (2010) Magmatism, tectonics, geodynamics of the Earth. Nauka, Moscow, p 615

Bureau H, Keppler H (1999) Complete miscibility between silicate melts and hydrous fluids in the upper mantle: experimental evidence and geochemical implications. Earth Planet Sci Lett 165:187–196

Dasgupta R, Hirschmann MM, Dellas N (2005) The effect of bulk composition on the solidus of carbonated eclogite from partial melting experiments at 3 GPa. Contrib Mineral Petrol 149:288–305

Gorbachev NS (1990) Fluid-magma interaction in sulfide-silicate systems. Int Geol Rev 32(8):749–831

Gorbachev NS (2000) Supercritical state in the hydrous mantle: evidence from experimental study of fluid-bearing peridotite at $P = 40$ kbar and $T = 1400$ °C. Dokl Akad Nauk SSSR 370:147–150

Gorbachev NS, Kostyuk AV, Shapovalov YB, (2015a) Experimental study of the peridotite-H_2O system at $P = 3.8$–4 GPa, $T = 1000$–1400 °C: critical relations and vertical zoning of the upper mantle. Dokl Earth Sci 461(2):360–363

Gorbachev NS, Kostyuk AV, Shapovalov YB (2015b) Experimental study of the basalt–carbonate–H_2O system at 4 GPa and 1100–1300 °C: origin of carbonatitic and high-K silicate magmas. Dokl Earth Sci 464(2):1018–1022

Keppler H, Audetat A (2005) Fluid-mineral interaction at high pressure. Mineral behavior at extreme conditions. EMU Notes Mineral 7:225–251

Kessel R, Ulmer P, Pettke T, Schmidt MW, Thompson AB (2005) The water-basalt system at 4–6 GPa: Phase relations and second critical endpoint in a K-free eclogite at 700–1400 °C. Earth Planet Sci Lett 237:873–892

Kiseeva E, Yaksley GM, Hermann J, Litasov KD, Rosenthal A, Kamenetsky VS (2012) An experimental study of carbonated eclogite at 3.5–5.5 GPa—implications for silicate and carbonate metasomatism in the cratonic mantle. Journal of Petrol 53(4):727–759

Klein-BenDavid O, Izraeli ES, Hauri E, Navon O (2007) Fluid inclusions in diamonds from the Diavik mine, Canada and the evolution of diamond-forming fluids. Geochim Cosmochim Acta 71:723–744

Litasov KD, Ohtani E (2007) Effect of mater on the phase relations in Earth’s mantle and deep water cycle. Special paper Geol Soc of Amer 421:115–156

Litvin YuA (1991) Physical and chemical studies of the melting of the Earth’s deep matter. Nauka, Moscow, p 312

Mallik A, Dasgupta R (2012) Reaction between MORB-eclogite derived melts and fertile peridotite and generation of ocean island basalts. Earth Planet Sci Lett 329(330):97–108

Mibe K, Kanzaki M, Kawamoto T, Matsukage KN, Fei Y, Ono S (2007) Second critical endpoint in the peridotite–H_2O system. J Geophys Res 112:B03201

Navon O, Hutcheon ID, Rossman GR, Wasserburg GJ (1988) Mantle–derived fluids in diamond microinclusions. Nature 335:784–789

Stalder R, Ulmer P, Thompson AB, Gunther D (2001) High pressure fluids in the system MgO–SiO_2–H_2O under upper mantle conditions. Contrib Miner Petrol 140:607–618

Taylor LA, Neal CR (1989) Eclogites with oceanic crustal and mantle signatures from the Bellsbank kimberlite, South Africa, part 1: mineralogy, petrography, and whole rock chemistry. J Geol 97:551–567

Tumiati S, Fumagalli P, Tiraboschi C, Poli S (2013) An experimental study on COH-bearing peridotite up to 3.2 GPa and implications for crust-mantle recycling. J Petrol 54:453–479

Weiss Y, Kessel R, Griffin WL, Kiflawi I, Klein–BenDavid O, Bell DR, Harris JW, Navon O (2009) A new model for the evolution of diamond–forming fluids: Evidence from microinclusion–bearing diamonds from Kankan, Guinea. Lithos 112(2):660–674

Wyllie PJ, Rhyabchikov ID (2000) Volatile components, magmas, and critical fluids in upwelling mantle. J Petrol 41:1195–1206

Yaxley GM (2000) Experimental study of the phase and melting relations of homogeneous basalt plus peridotite mixtures and implications for the petrogenesis of flood basalts. Contrib Mineral Petrol 139:326–338